0026-895X/02/6203-618–627$7.00
MOLECULAR PHARMACOLOGY
Copyright © 2002 The American Society for Pharmacology and Experimental Therapeutics
Mol Pharmacol 62:618–627, 2002

Vol. 62, No. 3
1731/1002909
Printed in U.S.A.

A Reevaluation of Neuronal Zinc Measurements: Artifacts Associated with High Intracellular Dye Concentration

KIRK E. DINELEY, LATHA M. MALAIYANDI, and IAN J. REYNOLDS

Department of Pharmacology, University of Pittsburgh, Pittsburgh, Pennsylvania

Received March 14, 2002; accepted May 21, 2002

This article is available online at http://molpharm.aspetjournals.org

ABSTRACT

The emergence of zinc as a potent neurotoxin has prompted the development of techniques suitable for the measurement of intracellular free zinc ($[Zn^{2+}]_i$) in cultured cells. Accordingly, a new family of Zn^{2+}-sensitive fluorophores has become available. Using ionophore-induced elevations of $[Zn^{2+}]_i$ in cultured neurons, we measured $[Zn^{2+}]_i$-induced changes in the novel dyes FuraZin-1 and FluoZin-2 and compared them with the established $[Zn^{2+}]_i$-sensitive fluorophores mag-fura-2 and Newport Green. All of these dyes effectively detected $[Zn^{2+}]_i$, and FuraZin-1, FluoZin-2, and Newport Green showed selectivity for $[Zn^{2+}]_i$ over $[Ca^{2+}]_i$ and $[Mg^{2+}]_i$. However, the dyes showed little difference in their apparent sensitivity to $[Zn^{2+}]_i$, even though their in vitro affinities for Zn^{2+} varied from 20 nM to 3 μM. We show herein that this is a consequence of the relatively high concentrations of intracellular dye used in experiments of this nature. Thus, for the measurement of $[Zn^{2+}]_i$, the sensitivity of the reporting system is dominated by the intracellular dye concentration, whereas dye affinity is unimportant. We extend these findings to show that calibration of dye signal to ion concentration is critically dependent on precise measurement of intracellular dye concentration.

Long appreciated for its central role in fundamental cellular biochemistry, zinc is necessary for the proper function and regulation of a diverse array of biomolecules. Zinc serves in catalytic as well as structural roles for many proteins, is critical for lipid metabolism, and directly regulates gene expression and cell proliferation. Accordingly, human zinc deficiency is associated with a host of clinical abnormalities including growth retardation, suppressed immunity, and deteriorated mental capabilities (reviewed by Prasad, 1993).

Recently, the role of zinc in the central nervous system has received particular attention. Certain neurons accumulate large amounts of vesicularized zinc, and zinc modulates, at least in vitro, the activity of numerous channels, transporters, and receptors participatory in neural activity (Harrison and Gibbons, 1994). Perhaps most importantly, an expanding body of evidence shows zinc to be a potent neurotoxin. Excessive accumulation of intracellular zinc kills cultured neurons and glia (Choi and Koh, 1998). In animal models, zinc accumulates in neurons destined to die after ischemia, seizure, and blunt trauma (Frederickson et al., 1989; Koh et al., 1996; Suh et al., 2000). Although the precise source of zinc is currently debated, it is clear that these injury paradigms involve mobilization and redistribution of zinc already present in the brain, giving rise to its classification as an endogenous neurotoxin (Koh et al., 1996; Cuajungco and Lees, 1998; Lee et al., 2000).

The investigation of zinc-mediated cell death has prompted the development of methodologies for measuring intracellular free zinc ($[Zn^{2+}]_i$). Historically, probes used to detect tissue zinc required sample fixation (Frederickson, 1989). In live neurons, initial measurements of $[Zn^{2+}]_i$ employed fluorescent, ion-sensitive indicators closely related to fura-2 (Sensi et al., 1997; Cheng and Reynolds, 1998). Though famous for measuring $[Ca^{2+}]_i$ and $[Mg^{2+}]_i$, these indicators are in fact very sensitive to heavy metals, with affinities for Zn^{2+} ranging from 2 to 30 nM (Tsien, 1999). However, selective detection of $[Zn^{2+}]_i$ has typically necessitated exclusion of Ca^{2+} and/or Mg^{2+} from the extracellular buffer. The advent of the first Zn^{2+}-selective live-cell fluorophore, Newport Green DCF,[1] allowed straightforward measurement of $[Zn^{2+}]_i$ while minimizing confounding signal from other biologically important divalent cations (Canzoniero et al., 1999; Sensi et al., 1999; Aizenman et al., 2000). However, Newport Green is a single-wavelength fluorophore and unfortunately

This work was supported by National Institutes of Health grant NS34138 (to I.J.R.) and by predoctoral fellowships from the National Institutes of Health (to L.M.M.) and the American Heart Association (to K.E.D.).

[1] Two forms of Newport Green are available from Molecular Probes: Newport Green DCF (K_D, Zn^{2+} ~1 μM) and Newport Green PDX (K_D, Zn^{2+} ~30 μM). This report uses only Newport Green DCF, although we have on occasion dropped the "DCF" suffix for easier reading.

ABBREVIATIONS: $[Zn^{2+}]_i$, intracellular free Zn^{2+} concentration; $[Ca^{2+}]_i$, intracellular calcium concentration; $[Mg^{2+}]_i$, intracellular free Mg^{2+} concentration; AM, acetoxymethyl ester; HBSS, HEPES-buffered salt solution; TPEN, *N*,*N*,*N*′,*N*′-tetrakis(2-pyridalmethyl)ethylenediamine; pyr, pyrithione.

lacks advantages that popularized dual-wavelength (i.e., ratiometric) indicators, such as fura-2.

A new family of Zn^{2+} dyes may provide superior alternatives. These probes are modifications of pre-existing single- or dual-wavelength Ca^{2+} dyes, are available in cell-permeant forms, and have affinities for zinc in the micromolar range. In the present study, we initially evaluated properties of two of these novel indicators, FuraZin-1 and FluoZin-2, and compared them with the more established dyes Newport Green and mag-fura-2. Commercial data regarding fluorescent indicators can be misleading, because testing is almost always performed in spectrofluorometer-based, cell-free assays. Our comparisons therefore used fluorescence microscopy recordings from intact, dye-loaded neurons, a setting more consistent with their intended practical use. Our characterization of these dyes revealed that the high-affinity indicator mag-fura-2 (K_D, Zn^{2+} ~20 nM) displayed a sensitivity for $[Zn^{2+}]_i$ that was surprisingly similar to other indicators of much lower affinities (~1–3 μM). A reconsideration of ion-dye binding stoichiometry predicted that apparent dye sensitivity would in theory be heavily dominated by intracellular dye concentration rather than the affinity constant. We tested this principle in neurons containing different concentrations of mag-fura-2. In agreement with modeling predictions, dye saturation in neurons varied according to the intracellular dye concentration.

These results establish the utility of novel Zn^{2+}-sensitive indicators in the practical setting of fluorescence microscopy. Furthermore, we demonstrate that although dye-based estimations of $[Zn^{2+}]_i$ are misleading, calculations that consider intracellular dye concentration may allow accurate determination of the total Zn^{2+} load.

Materials and Methods

Cell Culture. All procedures using animals were in accordance with the National Institutes of Health Guide for the Care and Use of Laboratory Animals and were approved by the Institutional Animal Care and Use Committee of the University of Pittsburgh. Primary cultures of embryonic rat forebrain neurons were prepared as described previously (Brocard et al., 2001). Briefly, embryonic day 17 Sprague-Dawley rat fetuses were surgically removed from an anesthetized dam. Fetal forebrains were then excised, dissociated by trypsinization, and plated on poly-D-lysine–coated 31-mm glass coverslips in Dulbecco's modified Eagle's medium supplemented with 10% fetal bovine serum, penicillin (100 U/ml), and streptomycin (100 μg/ml). Twenty-four hours after plating, the medium was replaced with Dulbecco's modified Eagle's medium containing 10% horse serum in place of fetal bovine serum, and coverslips were inverted to inhibit proliferation of neuroglia. Neurons were kept in a 5% CO_2, 37°C incubator, and all experiments were performed after 9 to 16 days in culture.

Reagents and Solutions. All ion-sensitive fluorophores and *N*,*N*,*N*′,*N*′-tetrakis(2-pyridalmethyl)ethylenediamine (TPEN) were purchased from Molecular Probes (Eugene, OR); all other reagents were purchased from Sigma-Aldrich (St. Louis, MO) unless otherwise noted. During microfluorimetric measurements, coverslips were continuously superfused with HEPES-buffered salt solution (HBSS) containing 150 mM NaCl, 5 mM KCl, 0.9 mM $MgSO_4$, 1.4 mM $CaCl_2$, 20 mM HEPES, and 5.5 mM glucose, and adjusted to pH 7.4 with NaOH. When appropriate, Zn^{2+} was added to the buffer from a 1000× stock of $ZnCl_2$ in 25 mM HCl. The Zn^{2+}-specific ionophore sodium pyrithione (1-hydroxypyridine-2-thione) was added at a concentration of 20 μM from a 20 mM stock in dimethyl sulfoxide. To reduce $[Zn^{2+}]_i$, the membrane-permeant heavy metal chelator TPEN was included at a concentration of 25 or 50 μM from a 25 mM stock in dimethyl sulfoxide. Experiments addressing dye sensitivity to high $[Mg^{2+}]_i$ used HBSS containing high extracellular Mg^{2+} concentration (9 mM) as described previously (Stout et al., 1996).

Fluorescence Microscopy. Recordings were performed at room temperature (20–25°C). $[Zn^{2+}]_i$ was measured using the Zn^{2+}-sensitive fluorophores mag-fura-2, FuraZin-1, FluoZin-2, and Newport Green DCF. Figure 1 shows the structure, K_D for Zn^{2+}, and excitation and emission wavelengths for each dye. (The properties of FuraZin-1 and FluoZin-2 are described only in product information inserts, which can be found on the Molecular Probes website: http://www.molecularprobes.com.) To load neurons with cell-permeant dye derivatives, coverslips were incubated in 1 ml of HBSS containing 5 mg/ml of bovine serum albumin and 5 μM dye in the dark at 37°C. The incubation period was 20 min for mag-fura-2 and FuraZin-1 and 30 min for Newport Green and FluoZin-2. After loading, coverslips were rinsed thoroughly, mounted in a recording chamber, and superfused with HBSS at 10 ml/min at room temperature. For each coverslip, the responses of approximately 10 to 15 neurons were compiled to generate a single mean trace. The PC-based imaging system used in these experiments consisted of the following components: a Nikon Diaphot 300 microscope equipped with a 40× oil-immersion objective (Tokyo, Japan), a charge-coupled device camera (Hamamatsu Photonics, Hamamatsu City, Japan), a monochromator-driven xenon light source (ASI, Eugene, OR), and SimplePCI imaging software (Compix, Cranberry, PA). For simultaneous imaging of mag-fura-2 and Newport Green DCF, neurons were loaded with Newport Green (5 μM) for 30 min. Ten minutes later, 5 μM mag-fura-2 acetoxymethyl ester (AM) was added, and coincubation with both dyes continued for an additional 20 min.

Optical parameters used for the dyes were as follows: mag-fura-2 was alternately illuminated at 335 and 375 nm, and FuraZin-1 was similarly illuminated at 335 and 380 nm. For both dyes, light passed through a 400-nm dichromatic mirror and was adjusted by a 510 ± 40-nm bandpass emission filter. Newport Green and FluoZin-2 were excited at 490 nm, and light passed through a 515-nm dichromatic mirror and was adjusted by a 535 ± 12.5-nm bandpass emission filter. All optical components were purchased from Chroma Technology (Brattleboro, VT).

To determine intracellular excitation spectra in the presence of ambient $[Zn^{2+}]_i$, a coverslip of dye-loaded but otherwise unstimulated neurons in HBSS was placed on the microscope. The monochromator-driven xenon light source illuminated a field of 10 to 15 neurons over a wavelength range of up to 150 nm, in 2-nm increments, with the camera capturing a single exposure for each wavelength surveyed at a rate of 1 frame/s. Thus, the procedure required constant illumination of the cells for no more than 75 s. The coverslip was then treated with pyrithione and Zn^{2+} (20 and 300 μM, respectively) for 5 min to produce high $[Zn^{2+}]_i$. Immediately thereafter, the same neurons were again illuminated across the same range of wavelengths. The resultant images were used to generate a graph of mean fluorescence intensity versus wavelength under conditions of both basal and high $[Zn^{2+}]_i$.

Intraneuronal Dye Concentration. To determine the amount of intracellular dye accumulation in response to a known extracellular concentration of cell-permeant AM, three to six coverslips were exposed to varying concentrations of mag-fura-2 AM (0.1, 0.5, 1, 5, and 20 μM) for 20 min at 37°C in HBSS supplemented with bovine serum albumin. Newport Green DCF (5 μM for 30 min) and fura-2 AM (5 μM for 40 min) were also assayed. Using 1 to 1.5 ml of low ionic strength buffer (containing 120 mM KCl, 10 mM HEPES, and 0.2 mM EGTA, pH 7.2), neurons were lysed and collected using a rubber policeman. To ensure recovery of all intracellular dye, recovered material was subjected to three freeze/thaw cycles. Cellular particulate was then separated by centrifugation (10 min at 10,000*g*), and the dye-containing supernatant was decanted and its volume measured.

Known aliquots of cell-impermeant dye salt added to a quartz cuvette containing 1.5 ml of the KCl buffer described above were analyzed using a Shimadzu RF-5301 PC spectrofluorometer (Shimadzu Scientific Instruments, Columbia, MD). For mag-fura-2 and fura-2, an excitation spectrum ranging from 300 to 420 nm was obtained by illuminating the sample at 1-nm intervals while collecting emitted light at 510 nm. Fluorescence produced by excitation at 365 nm was used to generate a standard curve of fluorescence intensity versus dye concentration. With Newport Green DCF, excitation ranged from 400 to 520 nm, emitted light was observed at 525 nm, and intensity produced by 490 nm was used to generate the standard curve. Samples of cell-derived supernatant were then analyzed with the same parameters, thus the sample dye concentration could be inferred from the standard curve. EGTA (1 mM) was added to ensure that the dye spectrum was not altered by divalent cations, and quenching with 1 mM $CoCl_2$ was used to confirm that all neuron-derived mag-fura-2 was properly cleaved and activated. Protein concentration was estimated for both the dye-containing supernatant and the pellet (after solubilization with NaOH and sonication) using a microplate BCA protein assay (Pierce Chemical, Rockford, IL). This permitted the normalization of dye concentration to each milligram of protein. Estimating 2 μl cell volume per mg of protein (Kletzien et al., 1975), we were ultimately able to approximate the concentration of intracellular dye that accumulated in neurons after exposure to various concentrations of cell-permeant derivatives.

Statistics. All experiments were repeated on at least three different coverslips taken from three separate culture preparations. All data plots, modeling, and appropriate statistical analyses were generated using GraphPad Prism, version 3.0 (GraphPad Software, San Diego, CA).

Results

We first evaluated the properties of the new dyes to establish excitation and emission optima in cells (Fig. 2). Although in vitro spectra are available for these dyes (Molecular Probes product literature), it cannot be assumed that dyes will show identical spectroscopic and ion-binding properties in the cellular environment. (Here and in all subsequent usage, "in vitro" refers to cuvette-based, cell-free assays performed in a spectrofluorometer.) Accordingly, we loaded neurons with mag-fura-2, Newport Green DCF, FuraZin-1, and FluoZin-2 and obtained excitation spectra under basal conditions where $[Zn^{2+}]_i$ is very low. Excitation spectra were again obtained from the same neurons after they were exposed to high extracellular Zn^{2+} in the presence of the Zn^{2+}-selective ionophore pyrithione, a maneuver known to substantially elevate $[Zn^{2+}]_i$. From these experiments, we selected optimal excitation wavelengths for each dye. For mag-fura-2 and FuraZin-1, λ_1 was chosen at 335 and 340 nm, respectively. Fluorescence produced at these wavelengths was adequately higher than background under resting conditions, while still exhibiting a modest increase in response to high $[Zn^{2+}]_i$. For λ_2, 375 and 380 nm were chosen because they exhibited a large $[Zn^{2+}]_i$-induced decrease in fluorescence that remained sufficiently higher than background intensity (Fig. 2, A and C). In later figures, fluorescence values for mag-fura-2 and FuraZin-1 are shown in ratio form (i.e., λ_1/λ_2). For the single-wavelength indicators Newport Green and FluoZin-2, excitation at 490 nm gave modest fluores-

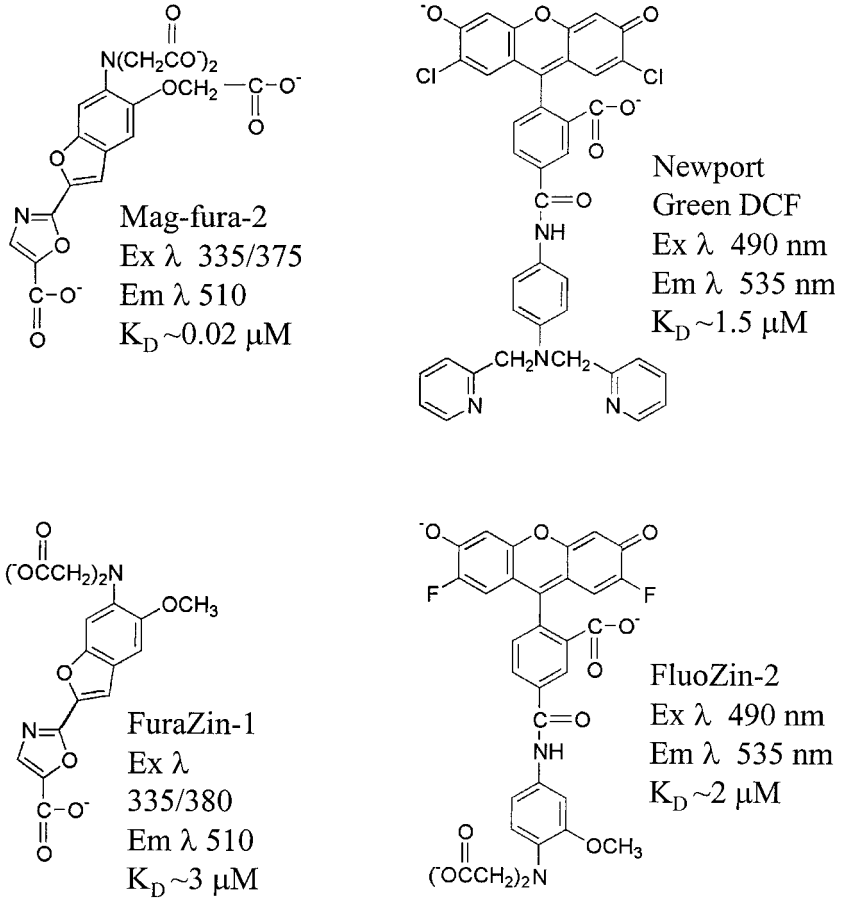

Fig. 1. Structures of Zn^{2+}-senstive dyes. The chemical structures of mag-fura-2, Newport Green DCF, FuraZin-1, and FluoZin-2 are accompanied by respective excitation and emission wavelengths employed in this manuscript. Also included for each dye is the reported affinity for Zn^{2+} (in micromolar). Note that mag-fura-2 and FuraZin-1 are ratiometric dyes, using two distinct excitation wavelengths. Newport Green DCF and FluoZin-2 are single-wavelength indicators.

cence under resting conditions while demonstrating several fold increases at high $[Zn^{2+}]_i$ conditions (Fig. 2, B and D). Newport Green and FluoZin-2 fluorescence is normalized to starting values (F/F_0) in later figures.

The utility of these dyes depends heavily on their selectivity for Zn^{2+} over other biologically relevant cations. Because these agents are derived from Ca^{2+} indicators, we first investigated their sensitivity to elevated $[Ca^{2+}]_i$ (Fig. 3). Our previous studies in neurons showed that very high $[Ca^{2+}]_i$ can be achieved by persistent activation of glutamate receptors (Stout and Reynolds, 1999). Exposing neurons to glutamate and the coagonist glycine (100 and 10 μM, respectively) elevates mag-fura-2 ratio values by 2- to 3-fold (Stout et al., 1998), consistent with the ability of mag-fura-2 to detect high $[Ca^{2+}]_i$. In contrast, activation of glutamate receptors did not increase Newport Green fluorescence (Fig. 3, A and D). Glutamate caused a slight increase in the FuraZin-1 ratio (~0.05 units; Fig. 3, B and E) and a 50% increase in normalized FluoZin-2 fluorescence. (Fig. 3, C and F). These changes might reflect a modest sensitivity to $[Ca^{2+}]_i$ or perhaps a $[Ca^{2+}]_i$-induced increase in $[Zn^{2+}]_i$. In any case, glutamate-induced changes in FuraZin-1 and FluoZin-2 were small relative to those elicited by Zn^{2+} and pyrithione (see Fig. 4). Therefore, it is reasonable to conclude that FuraZin-1 and FluoZin-2 are relatively insensitive to $[Ca^{2+}]_i$. We also examined dye sensitivity to $[Mg^{2+}]_i$ using an approach described previously (Stout et al., 1996). This method elevates $[Mg^{2+}]_i$ by 2 to 3 mM, which can be detected with mag-fura-2. However, under the same conditions, we observed no signal increase from either Newport Green, FuraZin-1, or FluoZin-2 (data not shown), demonstrating that these dyes are insensitive to $[Mg^{2+}]_i$.

We next evaluated dye responsiveness to elevated $[Zn^{2+}]_i$. Previously, we showed that pyrithione provides a useful way to deliver Zn^{2+} into neurons, elevating $[Zn^{2+}]_i$ in proportion to the extracellular Zn^{2+} concentration (Dineley et al., 2000). This approach allows characterization of dyes in terms of the minimum amount of added Zn^{2+} necessary to elicit a change in dye signal and also the amount of added Zn^{2+} that produces a maximal, or saturating, response. The minimum and maximum responses, as well as the general profile of the response, provide parameters that can be compared between dyes. One would predict that dyes of higher affinity would be more sensitive and saturate more quickly in response to lower concentrations of added Zn^{2+}, whereas dyes of lower affinity would be insensitive to low concentrations of added Zn^{2+} and saturate more slowly. Figure 4 shows typical traces from these experiments. In the case of each dye, the introduction of pyrithione alone had relatively little effect on the fluorescence signal, indicating that ambient Zn^{2+} in the buffer was low. Small signal increases were obtained by adding 0.3 μM Zn^{2+} to the extracellular solution, progressively larger responses resulted from 3 and then 30 μM added Zn^{2+}, and modest increments (if any) were encountered at 300 μM Zn^{2+}. For each indicator, addition of the high-affinity, membrane-permeant Zn^{2+} chelator TPEN re-

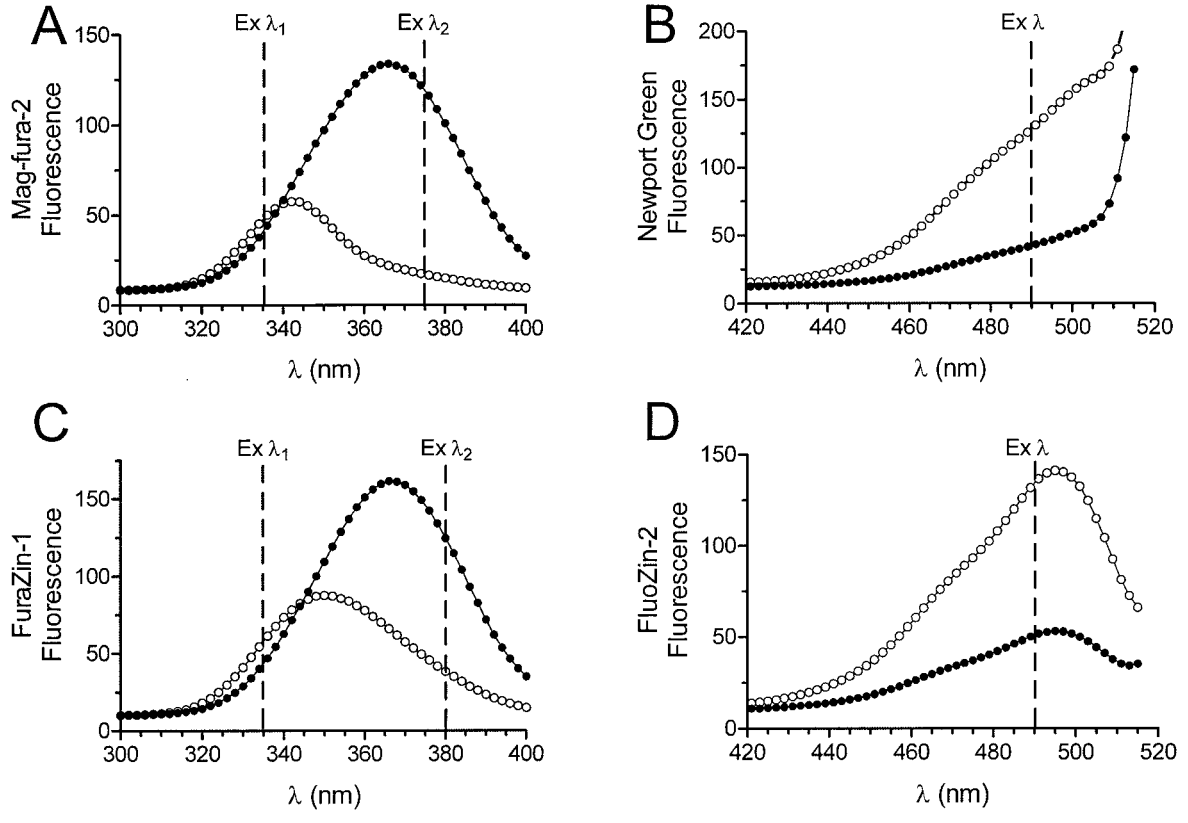

Fig. 2. Intracellular excitation spectra for Zn^{2+}-sensitive dyes acquired by fluorescence microscopy. Coverslips of neurons incubated with 5 μM cell-permeant forms of mag-fura-2 (A), Newport Green (B), FuraZin-1 (C), or FluoZin-2 (D) were illuminated through a range of excitation wavelengths at 2-nm intervals to establish excitation spectra in conditions of low $[Zn^{2+}]_i$ (●). Neurons were then stimulated with pyrithione (20 μM) and Zn^{2+} (300 μM) to produce high $[Zn^{2+}]_i$. The illumination procedure was then repeated to determine excitation spectra under conditions of high $[Zn^{2+}]_i$ (○). The vertical dashed lines correspond to the excitation wavelengths used for each dye in subsequent fluorescence microscopy experiments. (*See Materials and Methods* for experimental details.)

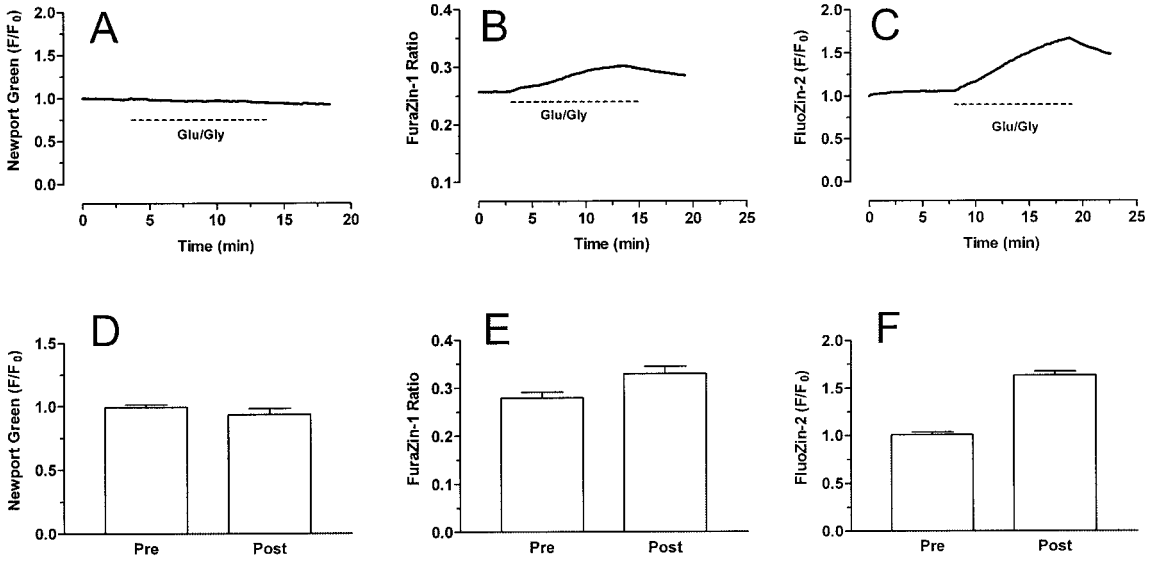

Fig. 3. $[Zn^{2+}]_i$-sensitive dyes are relatively insensitive to toxic levels of intracellular Ca^{2+}. Neurons incubated with 5 μM cell-permeant Newport Green (A), FuraZin-1 (B), or FluoZin-2 (C) were stimulated by glutamate (100 μM) with glycine (10 μM) for a 10-min period, as indicated by the dashed lines, to generate high $[Ca^{2+}]_i$. Respective summary data are presented in D, E, and F. Dye signal was taken before (Pre) and immediately after (Post) the glutamate + glycine stimulus, and bars represent mean ± S.E. For Newport Green (A and D) and FluoZin-2 (C and F), *y*-axis depicts normalized F/F_0 fluorescence values; for FuraZin-1 (B and E), *y*-axis depicts ratio values (λ_1/λ_2).

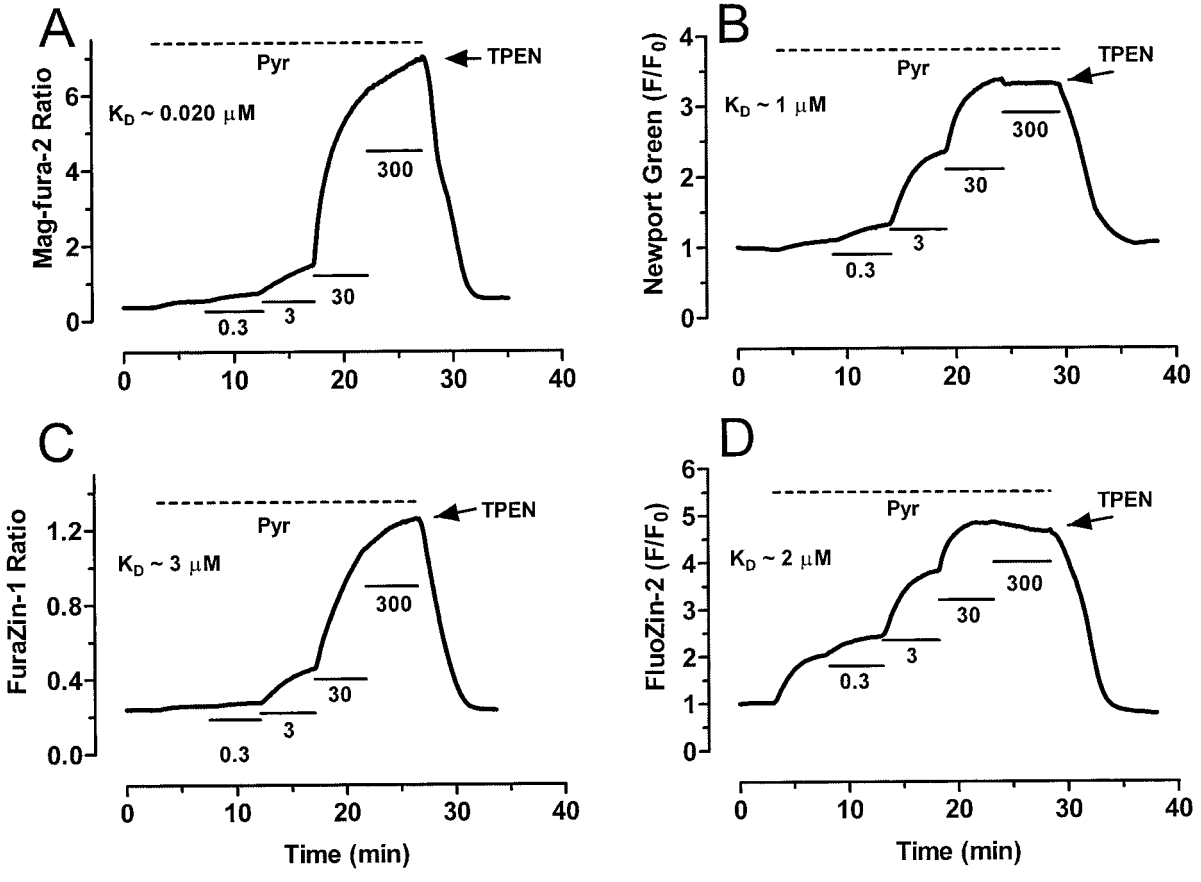

Fig. 4. $[Zn^{2+}]_i$-sensitive dyes exhibit similar response profiles, despite varying affinities for Zn^{2+}. Neurons incubated with 5 μM cell-permeant forms of mag-fura-2 (A), Newport Green (B), FuraZin-1 (C), or FluoZin-2 (D) were exposed to pyrithione (Pyr; 20 μM) in the presence of sequentially increased concentrations of added extracellular Zn^{2+} (0, 0.3, 3, 30, and 300 μM, each for 5 min) as indicated by the dashed and solid lines. Return of $[Zn^{2+}]_i$ to resting levels was achieved by addition of the high-affinity, membrane-permeant chelator TPEN (50 μM; starting at arrow). For the dual-wavelength dyes mag-fura-2 and FuraZin-1, ratio values are displayed on the *y*-axis; for the single-wavelength indicators Newport Green and FluoZin-2, dye signal is presented as normalized (F/F_0) fluorescence.

stored fluorescence signals to prestimulus values. The data from a number of these experiments are summarized in Fig. 5. It is surprising that all four of these dyes demonstrate very similar response profiles to the same series of Zn^{2+} stimuli, given that their in vitro affinities vary from 20 nM (mag-fura-2) to ~3 μM (FuraZin-1). (With respect to the *y*-axes, it should be noted that the fluorescence readout values for each dye will differ due to intrinsic differences in dye properties but that the general profiles of the responses are broadly similar between the dyes, regardless of *y*-axis scale.) Another set of experiments provided further confirmation. Neurons were coloaded with mag-fura-2 and Newport Green so that the responses of both dyes could be recorded simultaneously from the same neurons. Again, the response of the dyes was surprisingly similar given the ~100 fold difference between their in vitro affinities (Fig. 6).

These unexpected observations prompted us to reconsider the interpretation of these experiments. Interactions between dye and ion are governed by the principles of receptor-ligand binding. The saturation of dye by ion can be described by a standard receptor-ligand binding equation, which we have superficially modified so that "dye-ion" terminology is used instead of classic receptor-ligand parlance:

$$[dye \cdot ion] = \frac{[ion][dye_t]}{[ion] + K_D} \quad (1)$$

where [*ion*] represents the concentration of free Zn^{2+}, [dye_t] the concentration of free dye, [dye·ion] the concentration of dye·Zn^{2+} complex, and [K_D] the dissociation constant of the dye for Zn^{2+}. Indeed, it is a modification of this approach that was first proposed in the landmark paper by Grynkiewicz and colleagues (1985) and is widely used for calibrating Ca^{2+}-sensitive dyes. However, this approach assumes that 1) the quantity of ion bound to dye is insignificant compared with the total ion pool available and consequently 2) the formation of dye·ion complex does not appreciably deplete [*ion*]. However, high concentrations of intracellular dye are often achieved by the diffusion-limited dye-loading techniques employed in most live-cell fluorescence microscopy. In such experiments, sufficiently high dye concentrations will inevitably deplete [*ion*], thereby invalidating the above assumption. Fortunately, depletion of [*ion*] occurs in direct proportion to total intracellular dye concentration and can be accounted for with a modification to eq. 1 (Kenakin, 1993):

$$[dye \cdot ion] = \frac{([ion_t] - [dye \cdot ion])[dye_t]}{([ion_t] - [dye \cdot ion]) + K_D} \quad (2)$$

which is solved in eq. 3:

$$[dye \cdot ion] = \frac{1}{2}([ion_t] + K_D + [dye_t]) - \frac{1}{2}\sqrt{\{(-[ion_t] - K_D - [dye_t])^2 - 4[ion_t][dye_t]\}} \quad (3)$$

where [ion_t] represents the total ion concentration. It is apparent that the formation of dye·ion will be limited (saturable) as complex formation depletes available ion. When considering ion-induced changes in dye signal, it should be understood that the change in any dye signal will be propor-

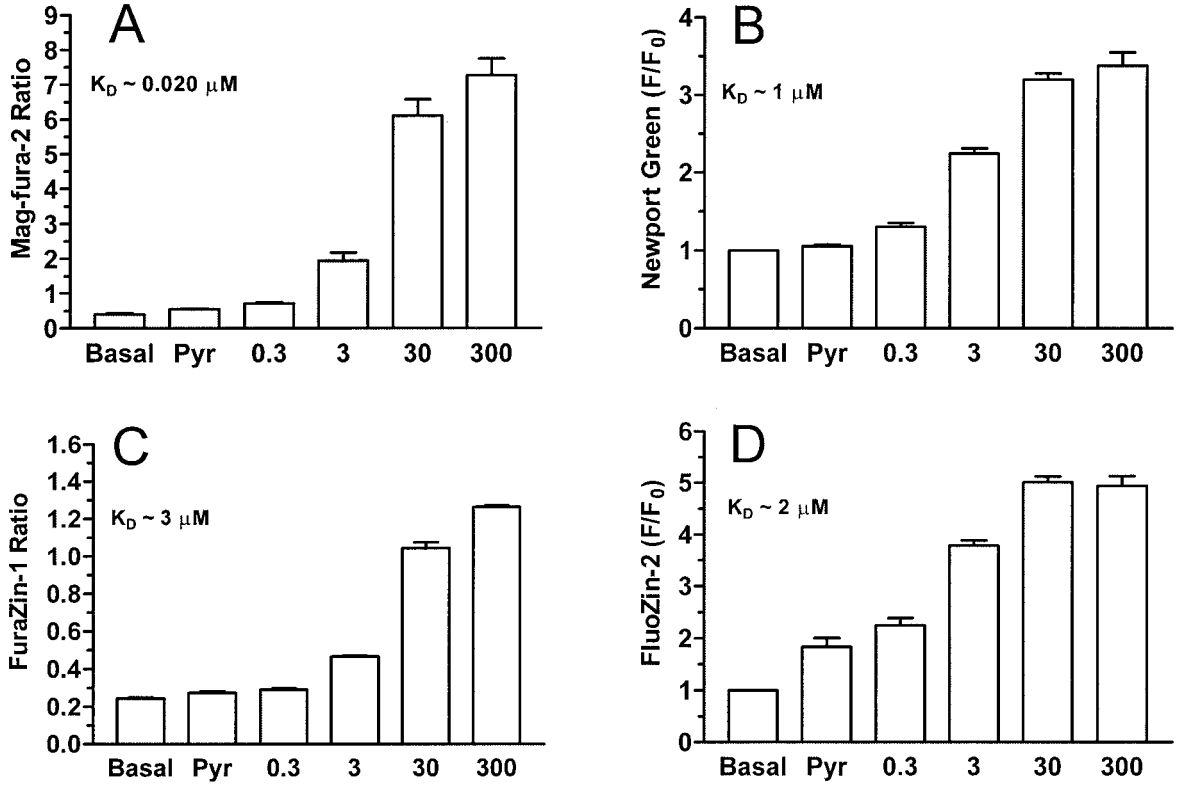

Fig. 5. $[Zn^{2+}]_i$ summary of $[Zn^{2+}]_i$-induced changes in Zn^{2+}-sensitive dyes. For each dye in Fig. 4, fluorescence values were taken during basal conditions and at the end of each 5-min stimulus (20 μM pyrithione alone and 20 μM pyrithione in the presence of 0.3, 3, 30, or 300 μM extracellular Zn^{2+}). For the dual-wavelength dyes mag-fura-2 and FuraZin-1, ratio values are displayed on the *y*-axis; for the single-wavelength indicators Newport Green and FluoZin-2, dye signal is presented as normalized (F/F_0) fluorescence. Bars represent mean ± S.E.

tional to the amount of dye·ion complex formed; that is, dye responses are a function of the fractional occupancy of the dye by ion. Using eq. 3, which accounts for ion depletion, we can predict fractional dye occupancy as a function of added ion under various dye concentrations. Figure 7 shows a series of such curves for a dye of fixed affinity for Zn^{2+} (20 nM; e.g., mag-fura-2) when [dye] is increased from 1 to 1000 μM. As is evident from this graph, dye concentration has a substantial impact on the sensitivity of the system, and each 10-fold increase in dye concentration causes a large rightward shift in the fractional occupancy curve. Figure 8 again uses eq. 3 in an alternative consideration: fractional occupancy curves are plotted for dyes with different Zn^{2+} affinities (20 nM-20 μM), whereas dye concentration remains fixed (which essentially models the comparisons made in this study). Figure 8A shows dyes of different affinity assuming 10 μM [dye], whereas Fig. 8B plots the same hypothetical dyes at a concentration of 1000 μM. The curves, barely discrete at 10 μM dye, are essentially superimposed at 1000 μM dye, regardless

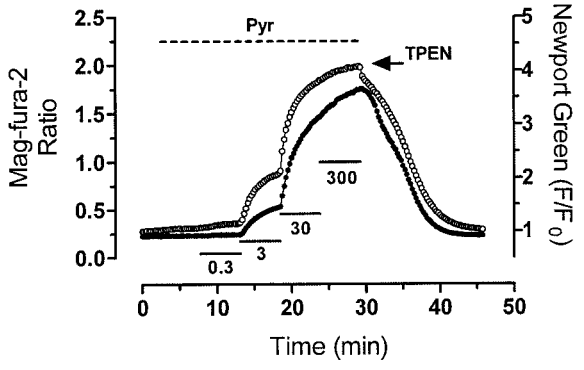

Fig. 6. Simultaneous recordings of mag-fura-2 and Newport Green. Neurons coloaded with cell-permeant Newport Green and mag-fura-2 (5 μM each) were exposed to pyrithione (Pyr; 20 μM) in the presence of sequentially increased concentrations of added extracellular Zn^{2+} (0, 0.3, 3, 30, and 300 μM, each for 5 min), as indicated by dashed and solid lines. At the end of the zinc treatment, TPEN (25 μM) was applied, beginning at (▼). Mag-fura-2 ratio values are represented by ● and displayed on the left *y*-axis, whereas normalized (F/F_0) Newport Green values are represented by ○ and displayed on the right *y*-axis. In comparing Fig. 6 with Fig. 4, the reader will notice different *y*-axis scale for mag-fura-2. The optics used for dual dye detection were different from those used to detect mag-fura-2 alone. The spectral bias of dual dye optics tends to compress the absolute range of the mag-fura-2 ratio. It should be emphasized, however, that the appropriate comparison involves the response profile rather than specific *y*-axis values.

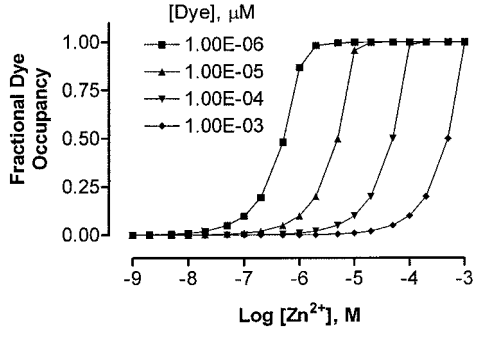

Fig. 7. Dye fractional occupancy corrected for intracellular dye concentration. Using eq. 3, and assuming a K_D for Zn^{2+} of 20 nM, theoretical fractional occupancy curves were generated for various intracellular dye concentrations (1, 10, 100, and 1000 μM). These curves model the saturation response of mag-fura-2 as a function of Zn^{2+}; increasing intracellular dye concentration results in a rightward shift.

of dye K_D. These surprising results show that dye response to ion fluxes is heavily dominated by the concentration of the dye itself, whereas K_D is virtually meaningless.

These results raise two important issues. First, intracellular dye concentration becomes a dominating parameter in evaluating the magnitude of the ion-induced dye responses. Second, the findings predict that the saturation characteristics of any dye should vary according to the intracellular dye concentration. We investigated both issues using mag-fura-2 because it is a well characterized dye that loads effectively into neurons, generating relatively bright fluorescence signals. However, there is little information available regarding the intracellular concentrations of mag-fura-2 following standard loading conditions. We incubated neurons with concentrations of mag-fura-2 AM between 0.1 and 20 μM, washed the cells carefully, lysed the neurons, and recovered the dye in the supernatant after centrifugation of cell debris. Using a standard curve generated with known concentrations of mag-fura-2 tetrapotassium salt, we estimated dye concentration in the recovered samples, which were then normalized to protein concentration (see *Materials and Methods*). Although we have been unable to directly measure the intracellular volume of neurons using radioisotope exclusion, volume in liver parenchymal cells has been estimated to be 2 μl/mg protein (Kletzien et al., 1975). Using this premise, calculated $[\text{mag-fura-2}]_i$ achieved millimolar concentrations (Fig. 9A). Proving that high intracellular dye concentrations are not unique to mag-fura-2, similar measurements with fura-2 and

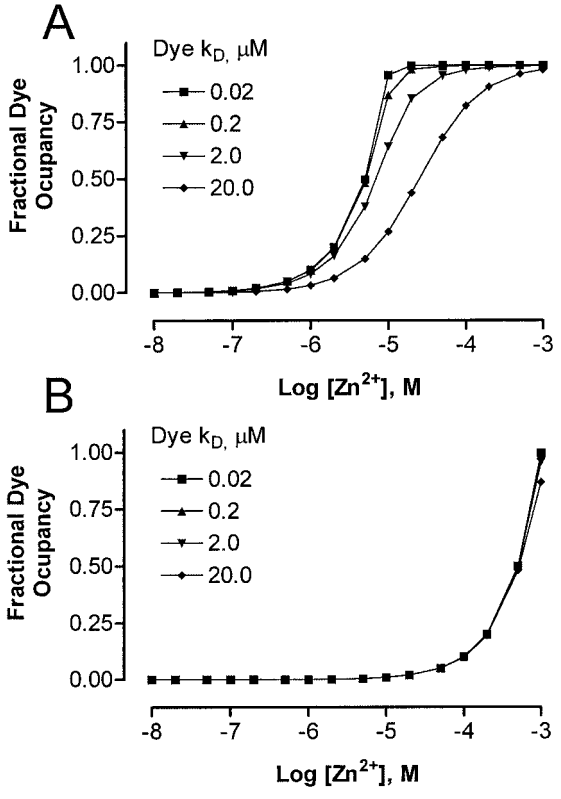

Fig. 8. High dye concentrations determine fractional occupancy of Zn^{2+}-sensitive dyes. Using eq. 3, theoretical fractional occupancy curves were generated for dyes of varying affinity (0.02, 0.2, 2.0, and 20 μM), each at a concentration of 10 μM (A). B presents similar data, but at a concentration of 1000 μM. Increasing dye concentration to millimolar levels results in virtually identical fractional occupancy, regardless of dye affinity.

Newport Green also approached or exceeded millimolar values (Fig. 9B). Using mag-fura-2 loading concentrations consistent with those of Fig. 9A, we repeated cell-based, fluorescence microscopy recordings where pyrithione was applied in the presence of sequentially increased extracellular Zn^{2+} concentration. The extent to which we were able to decrease intracellular dye concentration was essentially limited by the fluorescence-imaging hardware. Nevertheless, it was possible to test loading concentrations as low as 0.5 μM and up to 20 μM (Fig. 10A). Interestingly, neurons loaded with the least amount of dye showed the greatest sensitivity to the addition of chelator before the addition of Zn^{2+}. This suggests the presence of a finite pool of free intraneuronal Zn^{2+} or perhaps Zn^{2+} that the dye has leeched from internal binding sites. In either case, any signal from this relatively small amount of zinc is presumably obscured by high concentrations of intracellular dye. Most importantly, and as predicted by Fig. 7, neurons loaded with lower dye concentrations displayed greater Zn^{2+} sensitivity and saturated with less added Zn^{2+} compared with those loaded with higher dye concentrations. The results of several such experiments are summarized in Fig. 10B.

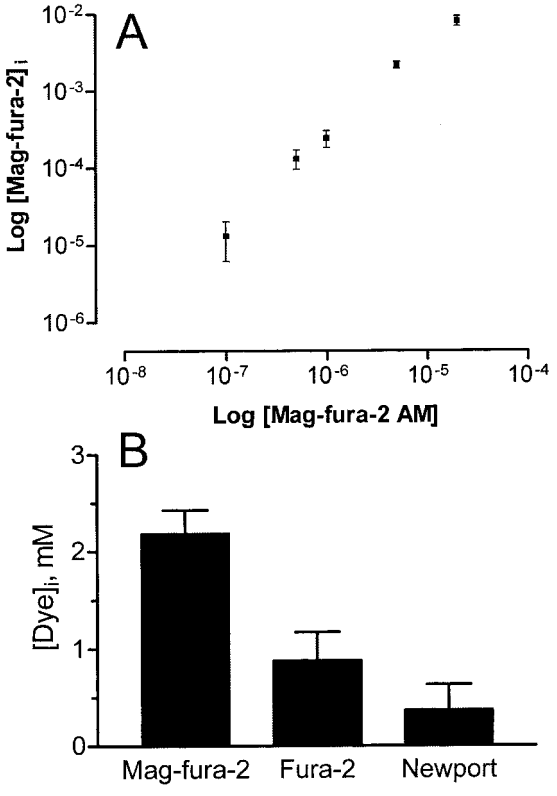

Fig. 9. Accumulation of intracellular dye in response to varied concentrations of extracellular AM. A presents intracellular mag-fura-2 concentration as a function of extracellular AM concentration. The soluble, dye-containing fraction was recovered from neurons incubated with varied mag-fura-2 AM concentrations (0.1, 0.5, 1, 5, and 20 μM) and analyzed for mag-fura-2 content using a spectrofluorometer (see *Materials and Methods*). Both axes plot molar dye concentration (M) on log10 scale. Data points are presented as mean ± S.E. B, comparison between different cell-permeant dyes. Similar to A, the soluble, dye-containing fraction was obtained from neurons incubated with 5 μM of either mag-fura-2, fura-2, or Newport Green and analyzed for dye content. Bars, depicting intracellular dye concentration in millimolar, are presented as mean ± S.E.

Discussion

In this study, we investigated the properties of several novel fluorescent dyes that may be suitable for measuring $[Zn^{2+}]_i$ in cells. We established that FuraZin-1 and FluoZin-2 respond to altered $[Zn^{2+}]_i$ and that their response is selective for $[Zn^{2+}]_i$ over $[Ca^{2+}]_i$ or $[Mg^{2+}]_i$. More importantly, these studies also revealed a surprising similarity in $[Zn^{2+}]_i$ sensitivity between dyes that have considerably different in vitro affinities for the ion. The apparent similarity between different dyes is the consequence of a poorly appreciated stoichiometric relationship between dye concentration and ion measurement that has a profound influence on the quantitative interpretation of intracellular ion signals. This issue becomes particularly important when using dyes of differing affinities and also when monitoring dye-ion interactions in which the ion has a high affinity for the dye.

Mag-fura-2 and Newport Green showed essentially identical sensitivities and saturation characteristics in cells. This prompted us to reassess conventional interpretation of dye signals. Using salts of the two dyes, we confirmed that their in vitro affinities were indeed very different (approximately 20 nM and 1 μM, respectively; data not shown). Our initial suspicion was that the intracellular environment caused one or both dyes to display altered properties. However, our data argued against this. First, high protein (bovine serum albumin) or lipid (cell membrane extracts) concentrations did not

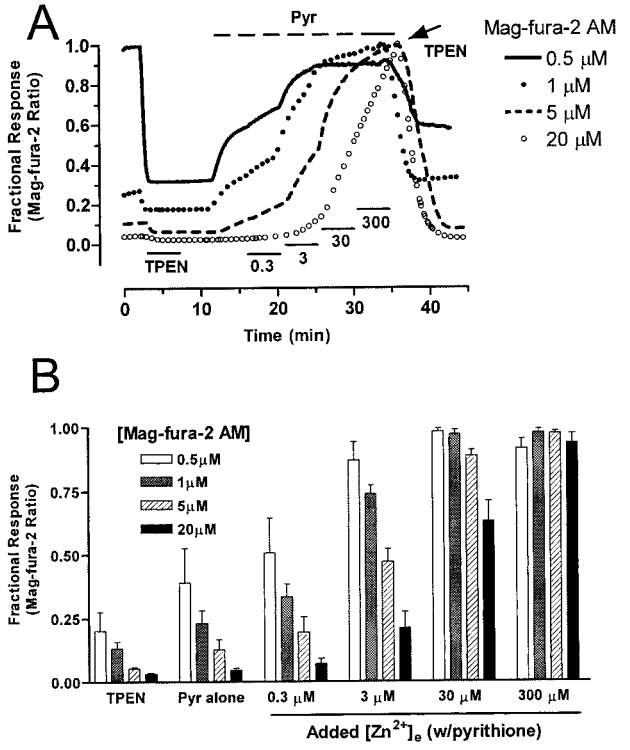

Fig. 10. Neurons incubated with different concentrations of mag-fura-2 AM display different Zn^{2+} saturation profiles. Neurons incubated with 0.5 (solid trace), 1 (●), 5 (dashes), or 20 μM (○) mag-fura-2 AM were treated with TPEN (50 μM) for 5 min, washed with normal HBSS for 10 min, then stimulated with pyrithione (Pyr; 20 μM) in the presence of sequentially increased concentrations of added extracellular Zn^{2+} (0, 0.3, 3, 30, and 300 μM, each for 5 min) as indicated by the dashed and solid lines (A). B, summary data from experiments shown in A. Mag-fura-2 ratio values obtained at the end of each 5-min stimulus are expressed as a fraction of the maximum ratio value observed in an individual experiment. Bars depict mean ± S.E.

affect dye characteristics in vitro. The addition of sucrose to increase viscosity also did not affect dye responsiveness. Finally, dye recovered from loaded neurons behaved identically to the purchased salt, arguing against some unexpected enzyme-mediated dye alteration.

Instead, different dyes respond similarly in cells because standard loading protocols achieve high concentrations of intracellular dye. The critical oversight involves the assumption that the total ion and free ion remain essentially equal in these experiments. This assumption is valid in most receptor-ligand applications, because the concentration of added ligand is in great excess compared with the number of available receptors in biological preparations. However, with $[ion]_i$ measurements, it is clear that levels of free ion can be substantially depleted by high concentrations of dye. Thus, although $[Zn^{2+}]_i$ may rise as high as a few hundred nanomolar in neurotoxic paradigms, $[dye]_i$ may approach or exceed millimolar values (Fig. 9). In these conditions, there will be substantial depletion of added Zn^{2+}. Equations 2 and 3 account for ion depletion; however, this correction reveals that dye·ion binding stoichiometry is determined by dye concentration, regardless of dye affinity for the ion of interest. This principle is illustrated in Figs. 7 and 8 and is experimentally validated in Fig. 10.

It is generally accepted that ion-induced changes in dye signal can be used to calculate absolute $[ion]_i$; it should be appreciated, however, that equations used for this purpose do not consider depletion of ion by excessive $[dye]_i$. Intracellular dye concentration is known precisely when the indicator is injected by micropipette (Helmchen et al., 1996). The vast majority of applications, however, use the diffusion-mediated loading approach employed in this report, and estimating $[dye]_i$ under these circumstances is much more difficult. We extracted soluble fractions from neuronal cultures and calculated cytoplasmic concentrations based on dye recovery. The dye concentrations we report might be compromised by a variety of factors. Most obvious is the parameter used to estimate cell volume (Kletzien et al., 1975). This estimate was not made in neurons, and it is likely that neurons with their many processes would yield a higher level of protein per unit volume. Such an error would lead to overestimated $[dye]_i$. Similarly, some dye may be sequestered in cellular compartments not accessible to ion influx. Our recovery methods would most likely liberate this pool of dye into the soluble fraction, again causing an overestimation of $[dye]_i$ available to interact with $[ion]_i$. We would note, however, that visual inspection of our fluorescence images yields no evidence of dye compartmentalization. Furthermore, prior studies support our estimates. Under broadly similar loading protocols, one report suggested that ~40 μM dye accumulated after loading with 5 μM fura-2 AM (Fink et al., 1998). Others reported millimolar concentrations using related fluorophores (Tsien, 1999). Indeed, it is generally accepted that loading with cell-permeant esters routinely yields a final $[dye]_i$ of 10 to 100 times the loading concentration (Haugland, 1996). Finally, we would emphasize that the modeling predictions presented in Figs. 7 and 8 use fairly conservative dye concentrations compared with actual $[dye]_i$ measurements shown in Fig. 9. Thus, our main conclusions would remain unaffected by even a 10-fold overestimation of $[dye]_i$.

Depletion of ion by high $[dye]_i$ is exacerbated when the indicator has a particularly high affinity for the ion of interest (e.g., when using mag-fura-2 to detect $[Zn^{2+}]_i$). Obviously, the dye will bind the ion very effectively, resulting in profound depletion of the free ion. It is generally recognized that an ideal fluorescent indicator should have a K_D near the anticipated concentration of the free ion. It is far less appreciated that $[dye]_i$ should also be in the same range as K_D. A useful guideline for illustrating potential ion depletion involves a quick ratio calculation of $[dye]_i/K_D$. Depletion must be accounted for once this value exceeds unity (i.e., the point at which $[dye]_i$ exceeds K_D) (Kenakin, 1993). In the case of Zn^{2+} and mag-fura-2, this ratio is exceedingly high, $>>10^3$ if one assumes $[dye]_i$ of 1 mM and K_D of 20 nM. With an affinity of 3 μM, a similar concentration of FuraZin-1 would still produce a ratio of $>10^2$. The detection of biologically relevant $[Zn^{2+}]_i$ necessitates high affinity, but affinity in turn dictates a concentration ceiling at which the fluorophore can be present without depleting free ion. For example, an ideal $[Zn^{2+}]_i$ indicator might exhibit an affinity of ~500 nM. However, $[dye]_i$ in excess of 500 nM will lead to considerable ion depletion. The issue now becomes one of practicality, as it is improbable that any $[Zn^{2+}]_i$ indicator could even be detected by fluorescence microscopy at $[dye]_i$ low enough to also avoid depletion of free ion. As our results show, reducing $[dye]_i$ is limited in practice by the detection capability of the recording system. In conclusion, it can now be stated that for any Zn^{2+}-sensitive dye, conversion of fluorescence to absolute $[Zn^{2+}]_i$ must account for Zn^{2+} depletion. These quantitative constraints, however, do not invalidate the use of these dyes for qualitative comparisons within and between cells.

The above considerations are also relevant to measurements of $[Ca^{2+}]_i$ and $[Mg^{2+}]_i$. Using fura-2 to detect $[Ca^{2+}]_i$, for example, $[dye]_i/K_D$ is still well in excess of 10^3 (assuming $[fura\text{-}2]_i = 250$ μM and $K_D = 140$ nM). Thus, depletion still confounds calculations of free ion concentrations. The effect is much smaller with very low-affinity Ca^{2+} indicators, so that the use of mag-fura-2 to measure $[Ca^{2+}]_i$ (K_D, Ca^{2+} ~50 μM) may be valid (Stout et al., 1998; Brocard et al., 2001). The problem disappears entirely when $[Mg^{2+}]_i$ is measured with mag-fura-2 (Stout et al., 1996), because the K_D for Mg^{2+} (0.5 mM) is very near our measured $[dye]_i$. It is also possible that comparisons between indicators of relatively similar affinities will be impacted more by differences in $[dye]_i$ than by slightly differing affinities. Conversely, the differences between high- and low-affinity Ca^{2+} indicators previously reported (Hyrc et al., 1997; Stout and Reynolds, 1999) might be erroneously exaggerated if the low-affinity indicator loads into cells more effectively (as seems to be the case for mag-fura-2).

The application of ion-sensitive indicators in biological systems is accompanied by strong motivation to convert fluorescence signals into precisely quantified intracellular ion concentrations. In this regard, ratiometric indicators, such as fura-2, are considered superior to their single-wavelength counterparts. In principle, variations in illumination intensity, specimen thickness, and dye concentration can be ignored when fluorescence intensities at two distinct wavelengths are ratioed. Because variations in these parameters affect both wavelengths proportionally, ratiometric tactics conveniently factor them out. It is now evident that dye concentration cannot be ignored, regardless of whether single-wavelength or ratiometric approach is used. It must be noted, however, that the pioneers of ratio imaging did not

intend for dye concentration to be ignored altogether; rather, their argument pertained to local variations of fluorophore concentration within a sample (Grynkiewicz et al., 1985). Those wishing to extrapolate precise values for intracellular ion concentrations have erroneously generalized this particular virtue of ratiometric imaging.

The key conclusion here is that it is difficult to infer $[Zn^{2+}]_i$, and probably $[Ca^{2+}]_i$, from the standard approaches to live-cell fluorescence microscopy. The solution to this problem is less clear. It is evident, however, that a critical parameter in these experiments is the intracellular dye concentration. If it is possible to determine $[dye]_i$ effectively, then the total ion flux in response to a stimulus could be estimated with some confidence. This parameter, together with the cytoplasmic volume, could then be used to approximate the intracellular ion concentration, provided that the impact of fixed intracellular buffers can be accounted for (Neher, 1995; Helmchen et al., 1996). Given that none of these parameters have yet been unequivocally established for Zn^{2+} in neurons, we feel that quantitative estimates of $[Zn^{2+}]_i$ are premature, even though this conclusion does not invalidate the approach for qualitative comparisons within or between cells.

Acknowledgments

We thank Geraldine Kress and Jennifer Fuhr for cell culture preparation and are grateful for helpful discussions provided by Rathna Malaiyandi, Drs. Elias Aizenman, Jacques Brocard, Rupa Mokkapatti, and Guillermo Romero and the Neurodegeneration Journal Club. We also appreciate the assistance of Geraldine Kress and Sam Park in generating Figs. 1 and 10, respectively.

References

Aizenman E, Stout AK, Hartnett KA, Dineley KE, McLaughlin B, and Reynolds IJ (2000) Induction of neuronal apoptosis by thiol oxidation: putative role of intracellular zinc release. *J Neurochem* **75:**1878–1888.

Brocard JB, Tassetto M, and Reynolds IJ (2001) Quantitative evaluation of mitochondrial calcium content in rat cortical neurones following a glutamate stimulus. *J Physiol (Lond)* **531:**793–805.

Canzoniero LMT, Turetsky DM, and Choi DW (1999) Measurement of intracellular free zinc concentrations accompanying zinc-induced neuronal death. *J Neurosci* **19:**1–6.

Cheng C and Reynolds IJ (1998) Calcium-sensitive fluorescent dyes can report increases in intracellular free zinc concentration in cultured forebrain neurons. *J Neurochem* **71:**2401–2410.

Choi DW and Koh JY (1998) Zinc and brain injury. *Annu Rev Neurosci* **21:**347–375.

Cuajungco MP and Lees GJ (1998) Nitric oxide generators produce accumulation of chelatable zinc in hippocampal neuronal perikarya. *Brain Res* **799:**118–129.

Dineley KE, Scanlon JM, Kress GJ, Stout AK, and Reynolds IJ (2000) Astrocytes are more resistant than neurons to the cytotoxic effects of increased $[Zn(^{2+})](i)$. *Neurobiol Dis* **7:**310–320.

Fink C, Morgan F, and Loew LM (1998) Intracellular fluorescent probe concentrations by confocal microscopy. *Biophys J* **75:**1648–1658.

Frederickson CJ (1989) Neurobiology of zinc and zinc-containing neurons. *Int Rev Neurobiol* **31:**145–238.

Frederickson CJ, Hernandez MD, and McGinty JF (1989) Translocation of zinc may contribute to seizure-induced death of neurons. *Brain Res* **480:**317–321.

Grynkiewicz G, Poenie M, and Tsien RY (1985) A new generation of Ca^{2+} indicators with greatly improved fluorescence properties. *J Biol Chem* **260:**3440–3450.

Harrison NL and Gibbons SJ (1994) Zn^{2+}: an endogenous modulator of ligand- and voltage-gated ion channels. *Neuropharmacology* **33:**935–952.

Haugland RP (1996) Indicators for Ca^{2+}, Mg^{2+}, Zn^{2+} and other metals, in *Handbook of Fluorescent Probes and Research Chemicals* pp 503–550, Molecular Probes, Eugene, OR.

Helmchen F, Imoto K, and Sakmann B (1996) Ca^{2+} buffering and action potential-evoked Ca^{2+} signaling in dendrites of pyramidal neurons. *Biophys J* **70:**1069–1081.

Hyrc K, Handran SD, Rothman SM, and Goldberg MP (1997) Ionized intracellular calcium concentration predicts excitotoxic neuronal death: observations with low-affinity fluorescent calcium indicators. *J Neurosci* **17:**6669–6677.

Kenakin T (1993) Radioligand Binding Experiments, in *Pharmacologic Analysis of Drug-Receptor Interaction*, pp 385–410, Raven, New York.

Kletzien RF, Pariza MW, Becker JE, and Potter VR (1975) A method using 3-*O*-methyl-D-glucose and phloretin for the determination of intracellular water space of cells in monolayer culture. *Anal Biochem* **68:**537–544.

Koh JY, Suh SW, Gwag BJ, He YY, Hsu CY, and Choi DW (1996) The role of zinc in selective neuronal death after transient global cerebral ischemia. *Science (Wash DC)* **272:**1013–1016.

Lee JY, Cole TB, Palmiter RD, and Koh JY (2000) Accumulation of zinc in degenerating hippocampal neurons of ZnT3-null mice after seizures: evidence against synaptic vesicle origin. *J Neurosci* **20:**RC79(1–5).

Neher E (1995) The use of fura-2 for estimating Ca buffers and Ca fluxes. *Neuropharmacology* **34:**1423–1442.

Prasad AS (1993) *Biochemstry of Zinc*. Plenum Press, New York.

Sensi SL, Canzoniero LM, Yu SP, Ying HS, Koh JY, Kerchner GA, and Choi DW (1997) Measurement of intracellular free zinc in living cortical neurons: routes of entry. *J Neurosci* **17:**9554–9564.

Sensi SL, Yin HZ, Carriedo SG, Rao SS, and Weiss JH (1999) Preferential Zn^{2+} influx through Ca^{2+}-permeable AMPA/kainate channels triggers prolonged mitochondrial superoxide production. *Proc Natl Acad Sci USA* **96:**2414–2419.

Stout AK and Reynolds IJ (1999) High-affinity calcium indicators underestimate increases in intracellular calcium concentrations associated with excitotoxic glutamate stimulations. *Neuroscience* **89:**91–100.

Stout AK, Li-Smerin Y, Johnson JW, and Reynolds IJ (1996) Mechanisms of glutamate-stimulated Mg^{2+} influx and subsequent Mg^{2+} efflux in rat forebrain neurones in culture. *J Physiol (Lond)* **492:**641–657.

Stout AK, Raphael HM, Kanterewicz BI, Klann E, and Reynolds IJ (1998) Glutamate-induced neuron death requires mitochondrial calcium uptake. *Nat Neurosci* **1:**366–373.

Suh SW, Chen JW, Motamedi M, Bell B, Listiak K, Pons NF, Danscher G, and Frederickson CJ (2000) Evidence that synaptically-released zinc contributes to neuronal injury after traumatic brain injury. *Brain Res* **852:**268–273.

Tsien RY (1999) Monitoring cell calcium, in *Calcium As a Cellular Regulator* (Carafoli E and Klee C eds) pp 28–54, Oxford University Press, New York.

Address correspondence to: Ian J. Reynolds, Department of Pharmacology, University of Pittsburgh, W1351 Biomedical Science Tower, Pittsburgh, PA 15261. E-mail: iannmda@pitt.edu